Inorganic Chemistry

ARTICLE

pubs.acs.org/IC

Lanthanide-Based Coordination Polymers Assembled from Derivatives of 3,5-Dihydroxy Benzoates: Syntheses, Crystal Structures, and Photophysical Properties

Sarika Sivakumar,[†] M. L. P. Reddy,*[,†] Alan H. Cowley,[‡] and Rachel R. Butorac[‡]

[†]Chemical Sciences and Technology Division, National Institute for Interdisciplinary Science & Technology (NIIST), CSIR, Thiruvananthapuram-695 019, India

[‡]Department of Chemistry and Biochemistry, The University of Texas at Austin, 1 University Station A5300, Austin, Texas 78712, United States

Supporting Information

ABSTRACT: Two new aromatic carboxylic acids, namely, 3,5-bis(benzyloxy)-benzoic acid (HL1) and 3,5-bis(pyridine-2-ylmethoxy)benzoic acid (HL2), have been prepared by replacing the hydroxyl hydrogens of 3,5-dihydroxy benzoic acid with benzyl and pyridyl moieties, respectively. The anions derived from HL1 and HL2 have been used for the support of a series of lanthanide coordination compounds [Eu^{3+} = **1**−**2**; Tb^{3+} = **3**−**4**; Gd^{3+} = **5**−**6**]. The new lanthanide complexes have been characterized on the basis of a variety of spectroscopic techniques in conjunction with an assessment of their photophysical properties. Lanthanide complexes **2**, **4**, and **6**, which were synthesized from 3,5-bis(pyridine-2-ylmethoxy)benzoic acid, were structurally authenticated by single-crystal X-ray diffraction. All three complexes were found to exist as infinite one-dimensional (1-D) coordination polymers with the general formula $\{[Ln(L2)_3\text{-}(H_2O)_2]\cdot xH_2O\}_n$. Scrutiny of the packing diagrams for **2**, **4**, and **6** revealed the existence of interesting two-dimensional molecular arrays held together by intermolecular hydrogen-bonding interactions. Furthermore, the coordinated benzoate ligands serve as efficient light harvesting chromophores. In the cases of **1**−**4**, the lowest energy maxima fall in the range 280−340 nm [molar absorption coefficient (ε) = (0.39−1.01) × 10^4 M^{-1} cm^{-1}]. Moreover, the Tb^{3+} complexes **3** and **4** exhibit bright green luminescence efficiencies in the solid state ($\Phi_{overall}$ = 60% for **3**; 27% for **4**) and possess longer excited state lifetimes than the other complexes (τ = 1.16 ms for **3**; 1.38 ms for **4**). In contrast to the foregoing, the Eu^{3+} complexes **1** and **2** feature poor luminescence efficiencies.

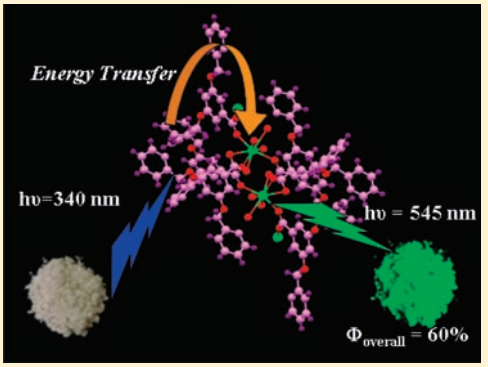

INTRODUCTION

Luminescent lanthanide coordination complexes display unique line-like emission bands, exhibit substantial Stokes shifts, possess very long luminescence lifetimes, and emit over the visible and near-IR (NIR) spectral domains. Depending on the particular lanthanide, complexes of this type offer numerous advantages in comparison with fluorescent organic compounds and other types of luminescent materials.[1] Furthermore, the fascinating photophysical properties of lanthanide complexes render them appropriate for a host of applications such as display devices, solid state lighting (including OLEDs), and sensors.[2] However, the spin- and parity-forbidden nature of the f-f transitions render direct photoexcitation of lanthanide ions disfavored. Accordingly, it is necessary to employ organic ligands to function as antennas by absorbing light and transferring this energy to the excited states of the central lanthanide ions.[3] The excited lanthanide ions then undergo radiative transitions to lower energy states which results in the characteristic multiple narrow band emissions. Since the emission intensity (brightness) and the color of the lanthanide emission both depend on the type of sensitizer employed, new sensitizing chromophores are highly sought after. As a consequence, a number of chromophoric antenna ligands have now been developed in an effort to achieve brighter Ln^{3+} luminescence. In this regard, the β-diketonate[4] and aromatic carboxylate ligands[5] have received the most attention.

Carboxylate anions are hard Lewis bases and are known to bind strongly to Ln^{3+} cations which possess a pronounced hard Lewis acid character.[6] Accordingly, lanthanide benzoates and their derivatives are stable and have attracted considerable attention for their potential use in a wide variety of fields on account of their novel luminescent and magnetic properties.[7−9] In particular, when modified with a light-harvesting groups, lanthanide benzoates have proved to be satisfactory luminescence sensitizers. In our recent work, it was demonstrated that replacement of the hydrogens of the $-NH_2$ moiety of amino benzoates by benzyl groups had a significant influence on the distribution of π-electron density within the ligand system and resulted in the development of a novel solid state photosensitizer

Received: January 19, 2011
Published: May 02, 2011

Table 1. Crystallographic and Refinement Data for 2, 4, and 6

	2	4	6
formula	$C_{57}H_{50}EuN_6O_{14.50}$	$C_{57}H_{53}TbN_6O_{16}$	$C_{57}H_{51}GdN_6O_{15}$
fw	1202.99	1236.97	1217.44
cryst sys	monoclinic	monoclinic	monoclinic
space group	*C*2/*c*	*C*2/*c*	*C*2/*c*
cryst size (mm^3)	0.12 × 0.11 × 0.06	0.27× 0.07 × 0.06	0.29× 0.04 × 0.04
temp/K	100(2)	293(2)	100(2)
a/(Å)	36.843(3)	36.52(3)	37.109(4)
b/(Å)	15.348(9)	15.555(14)	15.3430(14)
c/(Å)	9.890(6)	9.887(9)	9.8617(9)
α (deg)	90	90	90
β (deg)	101.133(9)	102.96(3)	99.711(4)
γ (deg)	90	90	90
V/Å^3	5487(5)	5473(8)	5534.4(9)
Z	4	4	4
D_{calcd}, g cm^{-1}	1.456	1.501	1.461
μ/(Mo, Kα) mm^{-1}	1.216	1.369	1.271
F(000)	2452	2520	2476
*R*1 [$I > 2\sigma(I)$]	0.1022	0.0991	0.0721
*wR*2[$I > 2\sigma(I)$]	0.2479	0.2457	0.1807
*R*1(all data)	0.1072	0.1050	0.0918
*wR*2(all data)	0.2515	0.2518	0.1915
GOF	1.715	1.139	1.259

for Tb^{3+} with an overall quantum yield of 82%.[10] It was also shown that the presence of an electron-donating methoxy group on position 3 of the 4-benzyloxy benzoic acid ligand resulted in a significant improvement in the photoluminescence efficiency ($\Phi_{overall}$ = 33%). For example, the Tb^{3+}-3-methoxy-4-benzyloxy benzoate complex has a $\Phi_{overall}$ value of 33% while that of the electron-withdrawing nitro-substituted Tb^{3+}-3-nitro-4-benzyloxy benzoate complex is only 0.1%.[5a] It has also been well documented that thiophenyl-substituted nitrobenzoic acid ligands are efficient sensitizers for both Eu^{3+} and Tb^{3+}.[6b]

Inspired by the efficient sensitization of various lanthanide benzoates, we have now designed and synthesized two new members of this ligand class, namely, 3,5-bis(benzyloxy)benzoic acid (HL1) and 3,5-bis(pyridine-2-ylmethoxy)benzoic acid (HL2). To enhance the antenna effects of the new benzoic acid ligands, the hydrogen atoms of 3,5-dihydroxy benzoic acid have been replaced by benzyl and pyridyl groups, respectively, and employed subsequently for the support of a series of new lanthanide complexes featuring Eu^{3+}, Gd^{3+}, or Tb^{3+} cations. The 3,5-bis(pyridine-2-ylmethoxy)benzoate complexes of Eu^{3+} (**2**), Gd^{3+} (**4**), and Tb^{3+} (**6**) were structurally authenticated by single-crystal X-ray diffraction. Unfortunately, it was not possible to grow suitable single crystals of the corresponding 3,5-bis(benzyloxy)benzoate complexes **1**, **3**, and **5**. However, these complexes were characterized satisfactorily on the basis of elemental analysis and FT-IR spectroscopy. The photophysical properties of all six new lanthanide benzoates have been explored and correlated with the electronic states of the newly designed ligands.

EXPERIMENTAL SECTION

Materials and Instrumentation. The following chemicals were procured commercially and used without subsequent purification: terbium(III) nitrate hexahydrate, 99.9% (Across Organics), 3,5-dihydroxy benzoic acid, 98% (Alfa Aesar), 2-bromomethyl pyridine hydrobromide, 98% (Aldrich), and benzyl bromide, 99.9% (Aldrich). All other chemicals used were of analytical reagent grade.

Elemental analyses were performed with a Perkin-Elmer Series 2 Elemental Analyzer 2400. A Perkin-Elmer Spectrum One FT-IR spectrometer using KBr (neat) was used to obtain the IR spectral data, and a Bruker 500 MHz NMR spectrometer was employed to record the ^{1}H NMR and ^{13}C NMR spectra of the ligands in DMSO-d_6 or D_2O solution. All mass spectra were recorded on a JEOL JSM 600 fast atom bombardment (FAB) high resolution mass spectrometer (FAB-MS), and the thermogravimetric analyses were performed on a TG/DTA-6200 instrument (SII Nano Technology Inc., Japan). X-ray diffraction (XRD) powder patterns were recorded in the 2θ range of 10−70° using Cu−K_α radiation (Philips X′pert). The absorbances of the ligands and complexes were measured in CH_3OH solution on a UV−vis spectrophotometer (Shimadzu, UV-2450), and the photoluminescence (PL) spectra were recorded on a Spex-Fluorolog FL22 spectrofluorimeter equipped with a double grating 0.22 m Spex 1680 monochromator and a 450W Xe lamp as the excitation source operating in the front face mode. The lifetime measurements were carried out at room temperature using a Spex 1040D phosphorimeter. The overall quantum yields ($\Phi_{overall}$) were measured by both absolute and relative methods as described elsewhere.[10−14]

The X-ray diffraction data were collected on a Rigaku AFC-12 Saturn 724+ CCD diffractometer equipped with a graphite-monochromated Mo Kα radiation source (λ = 0.71073 Å) and a Rigaku XStream low temperature device cooled to 100 K. Corrections were applied for Lorentz and polarization effects. The structure was solved by direct methods and refined by full-matrix least-squares cycles on F^2 using the Siemens SHELXTL PLUS 5.0 (PC) software package[15a] and PLATON.[15b] All non-hydrogen atoms were refined anisotropically, and the hydrogen atoms were placed in fixed, calculated positions using a riding model. Selected crystal data and data collection and refinement parameters are listed in Table 1. X-ray crystallographic information files can be obtained free of charge via www.ccdc.cam.ac.uk/consts/retrieving.html (or from CCDC, 12 Union Road, Cambridge CB2 1EZ, U.K.;

dx.doi.org/10.1021/ic2001249 |*Inorg. Chem.* 2011, 50, 4882–4891

Scheme 1. Synthetic Procedures for Ligands HL1 and HL2

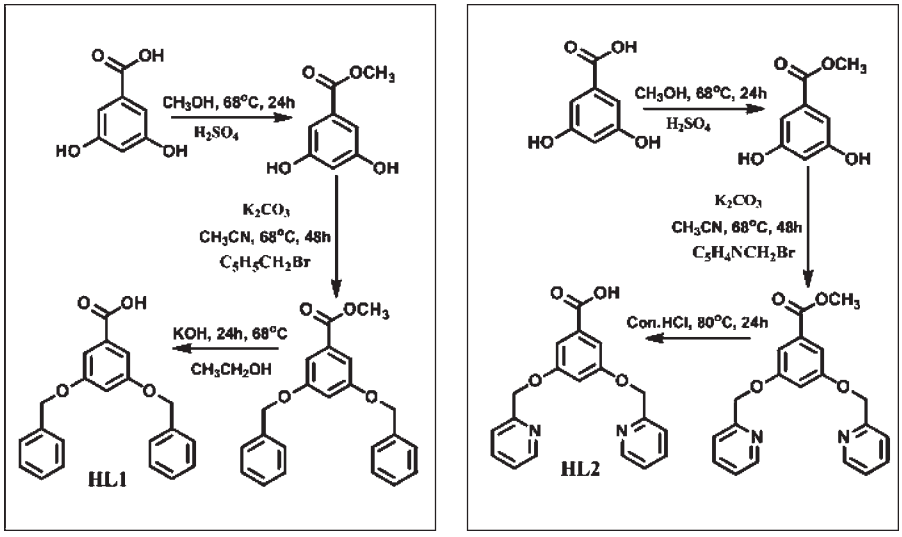

fax +44 1223 336033; e-mail deposit@ccdc.cam.ac.uk). The CCDC numbers are 789677, 789676, and 781131 for **2**, **4**, and **6**, respectively. Two of the pyridine moieties in complexes **2**, **4**, and **6** were found to be disordered by rotation about the oxygen−carbon bond. As a result, a series of constrained C−N and C−C bond lengths were employed to model the disorder along with bond angle restraints. The site occupancy factor of C14, C15, C16, C17, C18, C19, and N2 is refined to 63(2) % for **2**, **4**, and **6** and of C25, C26, C27, C28, C29, C30, and N2 is refined to 54(2) % for **2** and **6** and 62(2) % for **4**.

Synthesis of 3,5-Bis(benzyloxy)benzoic Acid (HL1). *(a). Synthesis of Methyl 3,5-Dihydroxybenzoate.* A methanolic solution of 3,5-dihydroxy benzoic acid (2.0 g, 13 mmol) was refluxed overnight in the presence of catalytic amounts of conc. H_2SO_4. The excess methanol was evaporated off, and the reaction mixture was poured into ice cold water. The resulting precipitate was filtered off, washed with water, and dried. Yield, 1.3 g (60%). ^{1}H NMR (500 MHz, $CDCl_3$): δ (ppm) 7.09 (s, 2H), 6.65 (s, 1H), 3.88 (s, 3H) . ^{13}C NMR (125 MHz, $CDCl_3$): δ (ppm) 167.24, 159.44, 133.07, 108.58, 107.90, 52.26. m/z = 169.14 $(M+H)^+$. FT-IR (KBr) ν_{max}: 3027, 1715, 1597, 1439, 1298, 1167, 1046, 764 cm^{-1}.

(b). Synthesis of Methyl 3,5-Bis(benzyloxy)benzoate. Methyl 3,5-dihydroxy benzoate (2.0 g, 12 mmol) was dissolved in 50 mL of freshly distilled acetonitrile and refluxed with potassium carbonate (8.0 g, 59 mmol) for 30 min. The resulting reaction mixture was further refluxed at 70 °C for 48 h following the addition of benzyl bromide (4.0 g, 24 mmol). The excess acetonitrile was then evaporated off, and the residual mixture was poured into ice cold water. Methyl 3,5-bis-(benzyloxy)benzoate was obtained as a white precipitate. Yield, 1.86 g (45%). ^{1}H NMR (500 MHz): δ (ppm) 7.43−7.37 (m, 8H), 7.35−7.32 (t, 2H, J = 7 Hz), 7.30−7.29 (d, 2H, J = 2 Hz), 6.81−6.80 (t, 1H, J = 2 Hz), 5.07 (s, 4H), 3.90 (s, 3H). ^{13}C NMR (125 MHz, $CDCl_3$): δ (ppm) 166.79, 159.81, 136.49, 132.08,128.65, 128.14, 127.59, 108.41, 107.28, 70.30, 52.29 . m/z = 349.40 $(M+H)^+$. FT-IR (KBr) ν_{max}: 3406, 2947, 2857, 1714, 1597, 1439, 1355, 1298, 1166, 841, 763 cm^{-1}.

Synthesis of 3,5-Bis(benzyloxy)benzoic Acid (HL1). 3,5-Bis-(benzyloxy)benzoate (2.0 g, 5.74 mmol) was refluxed for 24 h in the presence of KOH (0.97 g, 17.24 mmol) in 50 mL of ethanol. The reaction mixture was poured into ice cold water, acidified with dilute HCl, and the resulting precipitate was filtered, washed, dried, and recrystallized from ethanol. Yield, 1.80 g (94%). ^{1}H NMR (500 MHz): δ (ppm) 7.45−7.46 (d, 4H, J = 7 Hz), 7.39−7.41 (t, 4H, J = 7 Hz), 7.32−7.35 (t, 2H, J = 7 Hz), 7.16 (d, 2H, J = 2.5 Hz), 6.92−6.93 (t, 1H, J = 2.5 Hz), 5.15 (s, 4H). ^{13}C NMR (125 MHz, DMSO): δ (ppm) 166.88, 159.35, 136.64, 132.79, 128.45, 127.90, 127.63, 107.96, 106.50, 69.45. m/z = 335.46 $(M+H)^+$. Elemental analysis (%): Calcd for $C_{21}H_{18}O_4$ (334.12): C, 75.43; H, 5.43. Found: C, 74.75; H, 5.29. FT-IR (KBr) ν_{max}: 3038, 1693, 1596, 1446, 1422, 1378, 1301, 1167, 1030, 932, 852, 738, 695 cm^{-1}.

Synthesis of 3,5-Bis(pyridine-2-ylmethoxy)benzoic Acid (HL2). *(a). Methyl 3,5-Bis(pyridin-2-ylmethoxy)benzoate.* Methyl 3,5-dihydroxy benzoate (1.0 g, 6 mmol) was dissolved in 50 mL of freshly distilled acetonitrile and subsequently refluxed for 30 min with potassium carbonate (4.1 g, 30 mmol). The resulting reaction mixture was further refluxed at 80 °C for 48 h with 2-bromomethyl pyridine hydrobromide (3.0 g, 12 mmol). The excess acetonitrile was evaporated off, and the reaction mixture was poured into ice cold water. Methyl 3,5-bis-(pyridin-2-ylmethoxy)benzoate was obtained as a brown precipitate. Yield, 0.85 g (43%): ^{1}H NMR (500 MHz, acetone-d_6): δ (ppm) 8.58−8.59 (d, 2H, J = 5 Hz), 7.81−7.85 (m, 2H), 7.56−7.58 (d, 2H, J = 8 Hz), 7.31−7.34 (m, 2H), 7.27−7.28 (d, 2H, J = 2.50 Hz), 7.00−7.01 (t, 1H, J = 5 Hz), 5.25 (s, 4H), 3.87 (s, 3H). ^{13}C NMR (125 MHz, $CDCl_3$): δ (ppm) 166.59, 159.47, 156.59, 149.31, 136.90, 132.25, 122.79, 121.36, 108.72, 106.99, 70.86, 52.30 m/z = 350.93 $(M+H)^+$. FT-IR (KBr) ν_{max}: 3401, 1723, 1590, 1436, 1354, 1305, 1249, 1173, 1063, 840, 763 cm^{-1}.

(b). 3,5-Bis(pyridine-2-ylmethoxy)benzoic Acid (HL2). Methyl 3,5-bis(pyridin-2-ylmethoxy) benzoate (1.0 g, 3 mmol) was heated to reflux for 24 h in 50 mL of a 6 *M* HCl solution. The solution was concentrated to a volume of approximately 5 mL and stored at 5 °C. The resulting brown solid was filtered, dried, and recrystallized from CH_2Cl_2 to yield HL2·3HCl. Yield, 0.95 g (75%): ^{1}H NMR (500 MHz, D_2O): δ (ppm) 8.68−8.66 (d, 2H, J = 5.50 Hz), 8.49−8.51 (t, 2H, J = 7.75 Hz), 8.01−8.02 (d, 2H, J = 7.5 Hz), 7.91−7.94 (t, 2H, J = 6.75 Hz), 7.24 (s, 2H), 6.97 (s, 1H), 5.45 (s, 4H). ^{13}C NMR (125 MHz, DMSO-d6): δ (ppm) 166.42, 158.52, 152.29, 144.07, 143.58, 133.18, 125.39, 124.46, 108.69, 106.73, 66.99. m/z = 337.25 $(M+H)^+$ Elemental analysis (%): Calcd for $C_{19}H_{19}Cl_3N_2O_4$ (445.72): C, 51.20; H, 4.30; N, 6.28. Found: C, 51.57; H, 4.34; N, 6.20. FT-IR (KBr) ν_{max}: 3376, 1705, 1613, 1593, 1430, 1328, 1178, 1070, 759 cm^{-1}.

Syntheses of Lanthanide Complexes. In a typical procedure, an ethanolic solution of $Ln(NO_3)_3 \cdot 6H_2O$ (0.5 mmol) (Ln = Eu, Gd, or Tb) was added to a solution of the appropriate carboxylic acid (1.5 mmol) in ethanol in the presence of NaOH (1.5 mmol). Precipitation took place immediately, and each reaction mixture was stirred subsequently for 10 h at room temperature. The crude products were filtered, washed with ethanol, and dried. The resulting complexes were purified subsequently

dx.doi.org/10.1021/ic2001249 |*Inorg. Chem.* 2011, 50, 4882–4891

by recrystallization from ethanol. Single crystals of the lanthanide-3,5-bis(pyridine-2-ylmethoxy)benzoate complexes **2**, **4**, and **6** suitable for X-ray study were obtained from a dimethylsulfoxide/methanol solvent mixture after storage for 5 weeks at ambient temperature. However, efforts to grow single crystals of the lanthanide-3,5-bis(benzyloxy)benzoate complexes were not successful.

Eu(L1)$_3$(C_2H_5OH)(H_2O) (***1***). Elemental analysis (%): Calcd for $C_{65}H_{59}O_{14}Eu$ (1216.12): C, 64.20; H, 4.89. Found: C, 64.65; H, 4.85. FT-IR (KBr) ν_{max}: 3417, 1599, 1532, 1412,1378, 1215, 1156, 1054, 785 cm^{-1}.

[Eu(L2)$_3$(H_2O)$_2$]·0.5H_2O (***2***). Elemental analysis (%): Calcd for $C_{57}H_{50}N_6O_{14.50}Eu$ (1203): C, 56.91; H, 4.19; N, 6.99. Found: C, 56.72; H, 4.47; N, 6.81. FT-IR (KBr) ν_{max}: 3367, 1594, 1538, 1377,1414, 1287, 1161, 1063, 787 cm^{-1}.

Tb(L1)$_3$(C_2H_5OH)(H_2O) (***3***). Elemental analysis (%): Calcd for $C_{65}H_{59}O_{14}Tb$ (1223.08): C, 63.83; H, 4.86. Found: C, 63.61; H, 4.78 FT-IR (KBr) ν_{max}: 3373, 1597, 1538, 1416, 1378, 1212, 1157, 1054, 786 cm^{-1}.

[Tb(L2)$_3$(H_2O)$_2$]·2H_2O (***4***). Elemental analysis (%): Calcd for $C_{57}H_{53}N_6O_{16}Tb$ (1236.97): C, 55.34; H, 4.32; N, 6.79. Found: C, 55.44; H, 4.36; N, 6.67. FT-IR (KBr) ν_{max}: 3366, 1591, 1532, 1417, 1385, 1292, 1161, 990, 789 cm^{-1}.

Gd(L1)$_3$(C_2H_5OH)(H_2O) (***5***). Elemental analysis (%): Calcd for $C_{65}H_{59}O_{14}Gd$ (1221.41): C, 63.92; H, 4.87. Found: C, 63.69; H, 4.61. FT-IR (KBr) ν_{max}: 3398, 1599, 1532, 1415, 1379, 1207, 1157, 1055, 842, 786 cm^{-1}.

[Gd(L2)$_3$(H_2O)$_2$]·2H_2O (***6***). Elemental analysis (%): Calcd for $C_{57}H_{51}N_6O_{15}Gd$ (1217.44): C, 56.24; H, 4.22; N, 6.90. Found: C, 56.29; H, 3.85; N, 6.63. FT-IR (KBr) ν_{max}: 3324, 1591, 1539, 1413, 1375, 1295, 1161, 1062, 990, 787 cm^{-1}.

RESULTS AND DISCUSSION

Synthesis and Characterization of Ligands and Ln^{3+} Complexes 1−6. The ligands 3,5-bis(benzyloxy)benzoic acid (HL1) and 3,5-bis(pyridine-2-ylmethoxy)benzoic acid (HL2) were readily obtained in three steps starting from commercially available 3,5-dihydroxy benzoic acid as summarized in Scheme 1. The overall yields fell in the range 75−93%. The newly designed ligands were identified on the basis of ^1H and ^{13}C NMR spectroscopy (Supporting Information, Figures S1−S2), mass spectroscopy (FAB-MS), and elemental analysis. The protocols used for the syntheses of the lanthanide complexes are summarized in the Experimental Section. The elemental analysis data for the six complexes revealed that in each case the Ln^{3+} ion had reacted with the corresponding benzoic acid ligand in a metal-to-ligand mole ratio of 1:3. The FT-IR spectra of the ligands evidenced intense absorption bands characteristic of the carboxylate groups at ∼1440 and ∼1700 cm^{-1}, and are attributable to the symmetric ν_s(C═O) and asymmetric ν_{as}(C═O) vibrations, respectively. The bands centered at 1693 cm^{-1} (HL1) and 1705 cm^{-1} (HL2) in the spectra of the free ligands, which are assigned to stretching vibrations of the nonionized carboxylic groups, are shifted in the FT-IR spectra of **1**−**6**, thus confirming that the ligands are completely ionized, and hence in accord with the X-ray crystal structures. Moreover, the asymmetric and symmetric stretching vibration modes of the carboxylate groups in complexes **1**−**6** are further split into two peaks (Supporting Information, Table S1). The differences between the asymmetric and symmetric stretching vibration modes ($\Delta_{(C=O)}$ = ν_{as} − ν_s) fall in the ranges 206−221 and 115−126 cm^{-1}, which indicates that the carboxylate groups are coordinated to the Ln^{3+} ions in bidentate bridging and chelating modes.[16] A broad band observed above 3000 cm^{-1} (maximum at 3400 cm^{-1}) for complexes **1**−**6** is attributed to the characteristic ν(OH) stretching vibration and is indicative of the presence of water molecules.

Table 2. Selected Bond Lengths (Å) and Angles (deg) for Complexes 2, 4, and 6

2		4		6	
Eu1−Eu1	4.957	Tb1−Tb1	4.956	Gd1−Gd1	4.942
Eu1−O6	2.362(6)	Tb1−O1	2.345(6)	Gd1−O1	2.354(4)
Eu1−O1	2.371(7)	Tb1−O4	2.505(6)	Gd1−O4	2.498(4)
Eu1−O7	2.485(6)	Tb1−O6	2.313(5)	Gd1−O6	2.341(4)
Eu1−O4	2.492(6)	Tb1−O7	2.470(6)	Gd1−O7	2.485(4)
O6−Eu1−O6	144.0(3)	O6−Tb1−O6	145.6(3)	O6−Gd1−O6	144.3(2)
O6−Eu1−O1	103.4(2)	O6−Tb1−O1	85.3(2)	O6−Gd1−O1	85.4(15)
O1−Eu1−O1	154.1(3)	O1−Tb1−O1	154.9(3)	O1−Gd1−O1	153.1(2)
O6−Eu1−O7	71.7(2)	O6−Tb1−O7	71.7(2)	O6−Gd1−O7	71.5(15)
O1−Eu1−O7	79.0(2)	O1−Tb1−O7	80.0(2)	O1−Gd1−O7	80.3(16)
O7−Eu1−O7	73.3(3)	O7−Tb1−O7	71.9(3)	O7−Gd1−O7	73.3(2)
O6−Eu1−O4	70.5(2)	O6−Tb1−O4	70.9(2)	O6−Gd1−O4	70.6(15)
O1−Eu1−O4	77.7(2)	O1−Tb1−O4	76.9(2)	O1−Gd1−O4	78.2(15)
O7−Eu1−O4	129.9(2)	O7−Tb1−O4	129.96(19)	O7−Gd1−O4	130.3(13)

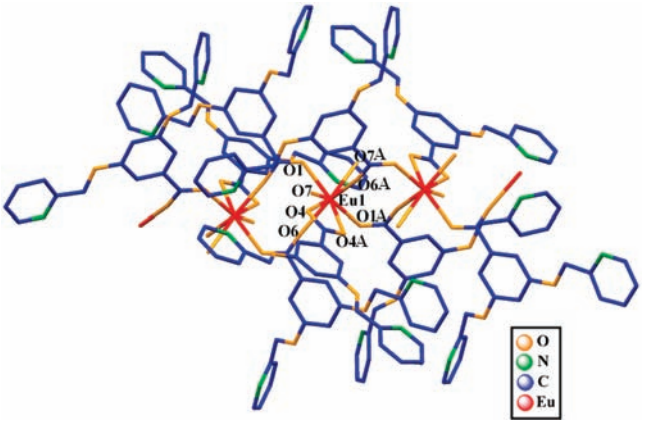

Figure 1. Capped stick model showing the coordination environment of **2**. All hydrogen atoms have been omitted for clarity. One − *x*, *y*, 3/2 − *z* completes the coordination sphere around Eu1. The Eu centers are related by an inversion center at 1/2, 1/2, 0. The complex extends infinitely along the *c* axis.

The thermal stabilities of complexes **1**−**6** were explored by means of thermogravimetric analyses (TGA) in the temperature range 30−800 °C. The thermograms exhibit similar features and the profiles are provided in the Supporting Information, Figure S3. All the compounds are thermally stable up to 300 °C. The onset of weight loss occurs between 220 and 260 °C (Found: 5.21% for compounds **1**, **3**, and **5** and 5.86% for compounds **2**, **4**, and **6**). These weight losses correspond to the release of coordinated water and solvent molecules (Calcd: 5.23% for compounds **1**, **3**, and **5** and 5.80% for compounds **2**, **4**, and **6**). The second weight loss occurs between 300 and 600 °C (Found: 81.01% for **1**, **3**, and **5** and 80.61% for **2**, **4**, and **6**) and is attributable to thermal decomposition of the organic components (Calcd: 81.75% for **1**, **3**, and **5** and 81.57% for **2**, **4**, and **6**) and corresponds to the formation of the stoichiometric amounts of Ln_2O_3 (Calcd ∼14%; Found ∼14%). In addition to the above weight losses, in the cases of compounds **2**, **4**, and **6** an initial weight loss of ∼1.5% was evident in the temperature range 105−110 °C, and is due to the elimination of lattice water molecules. The X-ray

dx.doi.org/10.1021/ic2001249 |*Inorg. Chem.* 2011, 50, 4882–4891

powder diffraction patterns for complexes **1**−**6** are similar to each other, thus implying that these compounds are isostructural (Supporting Information, Figure S4).

X-ray Crystal Structures of Ln^{3+}-3,5-bis(pyridine-2-ylmethoxy)benzoate Complexes 2, 4, and 6. Analysis of the single-crystal X-ray diffraction data for compounds **2**, **4**, and **6** reveals that these compounds are isostructural and consist of infinite one-dimensional (1-D) coordination polymers of the general formula $\{[Ln(L2)_3(H_2O)_2]\cdot xH_2O\}_n$. In view of the structural similarity of these complexes, detailed discussion is limited to the geometrical features of **2**. However, pertinent data collection parameters and a listing of significant bond distances and bond angles for all three complexes are provided in Tables 1 and 2, respectively. Compound **2** crystallizes in the monoclinic space group *C*2/*c*. The Eu1 center of **2** is coordinated to four carboxylate oxygen atoms of the bridging 3,5-bis(pyridine-2-ylmethoxy)benzoate ligands, two carboxylate oxygen atoms of the chelating benzoate ligand, and two water molecules (Figure 1). The analogous structures of **4** and **6** are presented in Supporting Information, Figures S5 and S7, respectively. The Eu1 center of **2** is surrounded by eight oxygen atoms in a distorted square antiprismatic arrangement with O−Eu1−O bond angles ranging from 70.5 to 154°. Furthermore, the Eu1 centers of **2** are doubly bridged by the carboxylate groups of the 3,5-bis(pyridine-2-ylmethoxy)benzoate ligands thereby forming an infinite 1-D chain (Figure 2). The carboxylate bridges also adopt a syn-anti conformation. The longest Eu1−O bonds involve the oxygen atoms of the bidentate chelating ligands [Eu1−O4: 2.492 Å], and the shortest such bonds are associated with the bridging carboxylate ligand [Eu1−O6: 2.362 Å; Eu1−O1: 2.371 Å].[17] As evident from Table 2, the distances between the adjacent metal centers are relatively large (∼5 Å) which is expected for $(\mu\text{-}\eta^1\text{:}\ \eta^1)_2$ bridges that contain four Ln-O interactions.[7b] Perhaps the most noteworthy structural feature of compounds **2**, **4**, and **6** is the presence of free Lewis basic pyridyl sites within the 1-D coordination polymer. In turn, this augurs well for the potential utility of these compounds for the recognition and sensing of metal ions.

Table 3. Selected Hydrogen-Bond Distances (Å) and Angles (deg) for Complexes 2, 4, and 6

compounds	contact type	H···A (Å)	D···A (Å)	D···H···A (deg)
2	C25−H25A···N2	2.689	3.536	145.60
4	C25−H25A···N2	2.697	3.556	147.69
6	C25−H25A···N2	2.619	3.476	147.51

A detailed analysis of the packing diagram of **2** reveals that the coordination polymers are connected by an intermolecular hydrogen bonding interaction between C25−H25A of a $-CH_2$ moiety and N2 of a pyridyl group with an H25A---N2 separation of 2.689 Å and an angle of 145.60° (Table 3) thus forming an infinite two-dimensional layered supermolecule[18] (Figure 3; see Supporting Information, Figure S6 for **4** and Supporting Information, Figure S8 for **6**).

Electronic States of the Ligands. The UV−visible absorption spectra of the free ligands and those of the corresponding Ln^{3+} complexes **1**−**6** were recorded in CH_3OH solution ($c = 2 \times 10^{-5}$ M) and are displayed in Figure 4. The trends in the absorption spectra of these complexes are identical to those observed for the free ligands, indicating that the singlet excited states of the ligands are not significantly affected by complexation to the Ln^{3+} ions. However, a small blue shift that is discernible in the absorption maxima of these complexes is attributed to the perturbation induced by metal coordination. The 3,5-bis(benzyloxy)benzoic acid ligand exhibits a broad band in the UV corresponding to a $^1\pi-\pi^*$ transition with a lowest energy maximum in the range 280−340 nm (λ_{max} = 307 nm) and a molar absorption coefficient (ε) of $1.01 \times 10^4\ M^{-1}\ cm^{-1}$. On the other hand, replacement of the hydrogen atoms of 3,5-dihydroxy benzoic acid by pyridyl moieties resulted in a blue shift of λ_{max} (302 nm), and a lower ε value ($3.90 \times 10^3\ M^{-1}\ cm^{-1}$) in comparison with that of 3,5-bis(benzyloxy)benzoic acid. The molar absorption coefficient values for complexes **1**−**6** were calculated at the respective λ_{max} values, and a summary of these data is presented in Supporting Information, Table S2. In general, the magnitudes of the molar absorption coefficients for the complexes are approximately three times higher than

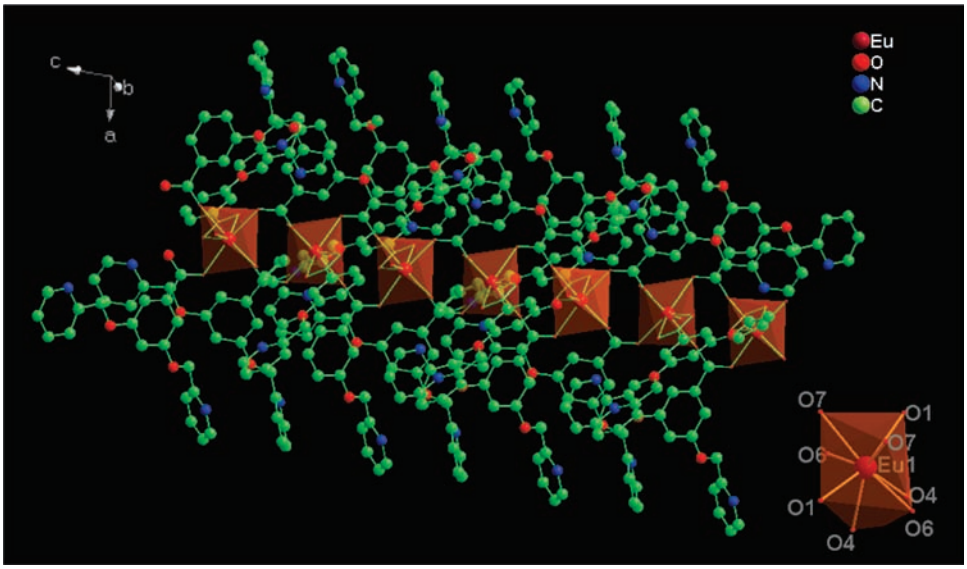

Figure 2. 1D coordination polymer chain of complex **2**.

dx.doi.org/10.1021/ic2001249 |*Inorg. Chem.* 2011, 50, 4882–4891

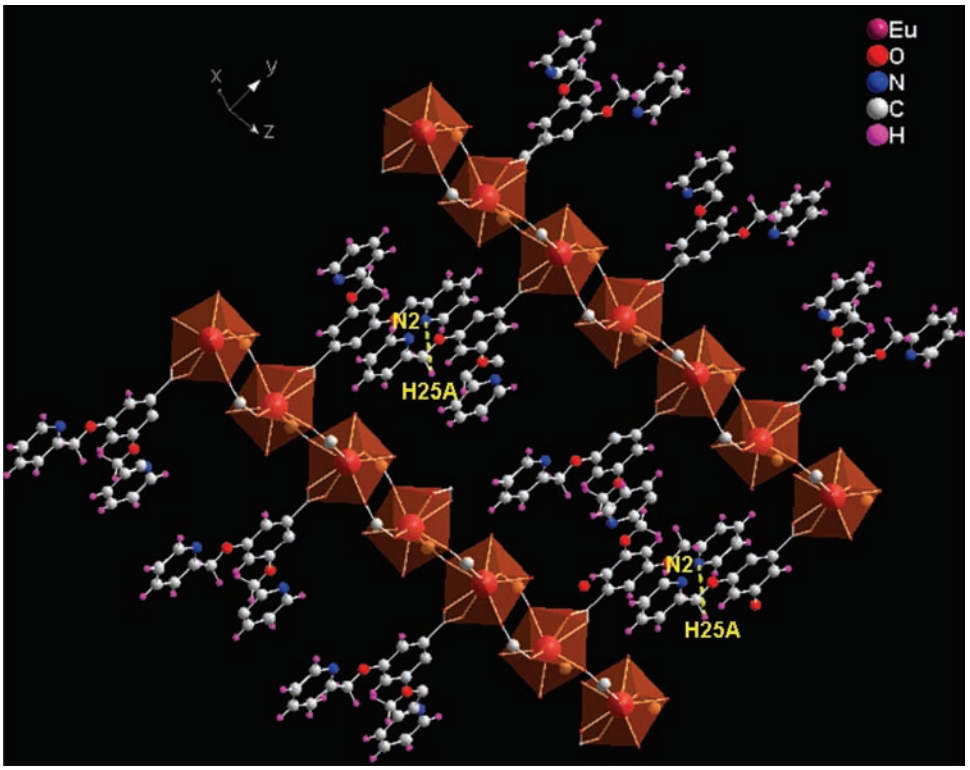

Figure 3. View of **2** showing the intermolecular hydrogen bonding interactions between C25−H25A of a CH_2 groups and N2 of the pyridyl moiety, where N2 is related by $x, -y, z - 1/2$. Some of the ligands have been omitted for clarity.

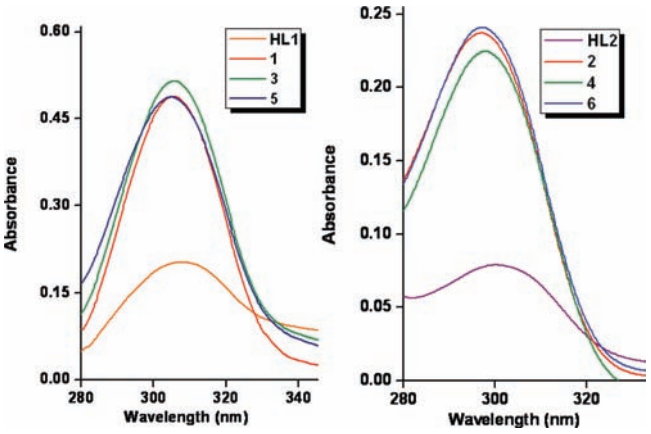

Figure 4. UV−visible absorption spectra for 3,5-bis(benzyloxy)benzoic acid (HL1), 3,5-bis(pyridine-2-ylmethoxy)benzoic acid (HL2), and complexes **1**−**6** in CH_3OH solution (2×10^{-5} M).

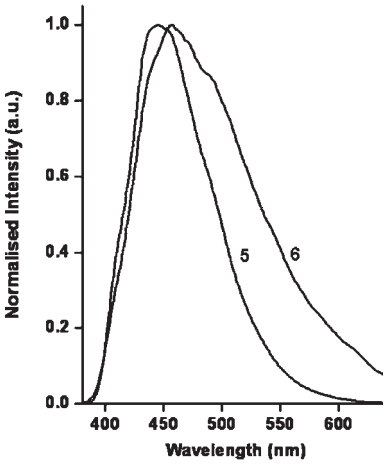

Figure 5. Phosphorescence spectra of gadolinium complexes **5** and **6** at 77 K.

those for the free ligands. Such a trend is consistent with the presence of three carboxylate ligands in each complex. It is also noteworthy that the large molar absorption coefficients observed for the new aromatic carboxylate ligands implies that they have a strong ability to absorb light.

For a ligand to serve as an effective photosensitizer, the first triplet state should be situated sufficiently above the emitting $^5D_0$ level of Eu^{3+} or the $^5D_4$ level of Tb^{3+} to permit efficient energy transfer to the higher excited states of the Ln^{3+} ions and thereby prevent quenching by back energy transfer processes.[19] In the present work, the triplet energy levels ($^3\pi\pi^*$) of the ligands have been estimated by reference to their lower wavelength emission edges (408 nm: 24509 cm^{-1}, 396 nm: 25253 cm^{-1} for ligands HL1 and HL2, respectively) of the low-temperature phosphorescence spectra of the Gd^{3+} complexes **5** and **6** (Figure 5). It is interesting to note that the triplet energy levels of the newly designed ligands lie well above the energies of the main emitting levels of $^5D_0$ for Eu^{3+} and $^5D_4$ for Tb^{3+}, thus indicating that these ligands can act as antennas for the photosensitization of trivalent Ln^{3+} ions. To elucidate the energy migration pathways in these Ln^{3+} complexes, it was also necessary to determine the singlet energy levels of the ligands. The singlet ($^1\pi\pi^*$) energy levels of

dx.doi.org/10.1021/ic2001249 |*Inorg. Chem.* 2011, 50, 4882–4891

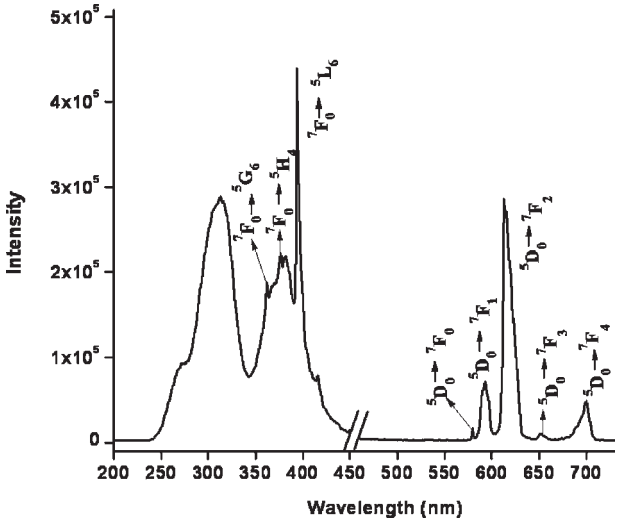

Figure 6. Room-temperature excitation and emission spectra for complex **1** (λ_{ex} = 316 nm) with emission monitored at approximately 612 nm.

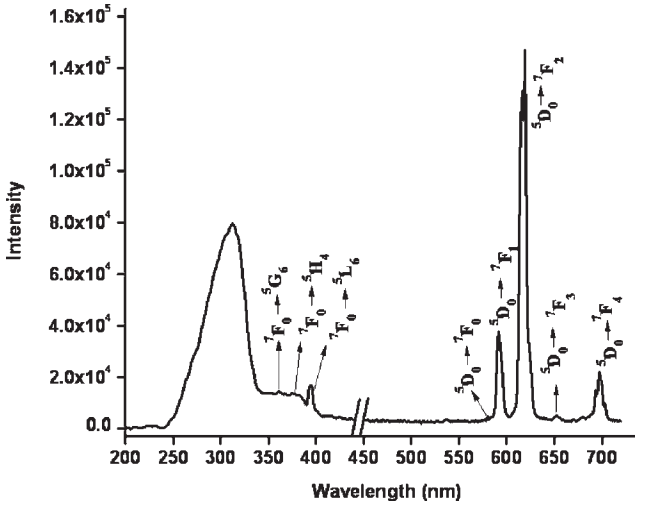

Figure 7. Room-temperature excitation and emission spectra for complex **2** (λ_{ex} = 313 nm) with emission monitored at approximately 612 nm.

these ligands were estimated by reference to the wavelengths of the UV−vis upper absorption edges of Gd^{3+} complexes **5** and **6** (Figure 4). The relevant values are 327 nm (30581 cm^{-1}) and 321 nm (31152 cm^{-1}) for HL1 and HL2, respectively. It is known that an efficient ligand-to-metal energy transfer requires a good $^1\pi\pi^* \rightarrow {}^3\pi\pi^*$ intersystem crossing, which is maximized when the energy difference between these states is close to 5000 cm^{-1}.[20] In our case, $\Delta E(^1\pi\pi^* - {}^3\pi\pi^*)$ it amounts to 6072 and 5899 cm^{-1} for ligands HL1 and HL2, respectively, and is therefore the designed ligands have good intersystem crossing efficiency.

Metal-Centered Luminescence. The Eu^{3+} and Tb^{3+} carboxylate complexes **1**−**4** presented in this study exhibit metal-centered luminescence. The combined excitation and emission spectra for the Eu^{3+} complexes **1** and **2** in the solid state at room temperature are presented in Figures 6 and 7, respectively. The excitation spectra for Eu^{3+} complexes **1** and **2** exhibit a broad band in the 250−350 nm region (centered at 310 nm) because of

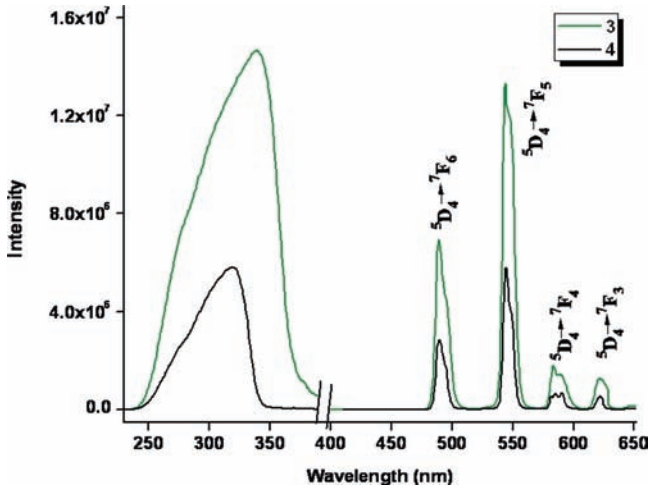

Figure 8. Room-temperature excitation and emission spectra for complexes **3** and **4** (λ_{ex} = 340, 320 nm respectively) with emission monitored at approximately 545 nm.

the $\pi-\pi^*$ transitions of the aromatic carboxylates. In addition, the excitation spectra of **1** and **2** display another broad band in the range 350−380 nm (centered at 360 nm) is overlapped by a series of sharp lines characteristic of the Eu^{3+} energy-level structure, and can be assigned to transitions between the $^7F_{0,1}$ and the $^5L_6$,$^5D_{3,2,1}$ levels.[21] Moreover these f-f transitions are more intense than the broad band observed related to the excited states of the 3,5-bis(benzyloxy)benzoic acid, which proves that luminescence sensitization via excitation of the ligand is not promising in **1**. On the other hand, in the excitation spectrum of Eu^{3+} complex **2**, the weaker signals observed in the 350−425 nm region arise from the f-f absorption of the Eu^{3+}cation, unequivocally proving the indirect excitation of the lanthanide centers via a typical antenna effect involving the organic ligand, bis-(pyridine-2-ylmethoxy)benzoic acid.

Under ligand excitation, the emission spectra of the europium complexes **1** and **2** (Figures 6 and 7) exhibit characteristic sharp bands of the metal ion in the 580−720 nm spectral range.[22] The intensity of the $^5D_0 \rightarrow {}^7F_2$ transition (electric dipole) is greater than that of the $^5D_0 \rightarrow {}^7F_1$ transition (magnetic dipole), which indicates that the coordination environment of the Eu^{3+} ions in **1** and **2** is devoid of an inversion center.[23] Furthermore, the absence of $\pi-\pi^*$ transitions of the ligands were evident in the emission spectra, which is typically diagnostic of the sensitization of the ligand toward the europium ion. To understand more about this phenomenon, the emission spectrum of the europium complexes **1** and **2** were also investigated by exciting at different f-f absorption of the Eu^{3+}cation, and the results are summarized in Supporting Information, Figure S9. At a 394 nm excitation wavelength (more intense line of europium absorption), the emission intensity of the $^5D_0 \rightarrow {}^7F_2$ transition (612 nm) is approximately 1.2 times more intense than when excited at 316 nm (ligand excitation), implying that ligand-to-europium energy transfer is not effective in the case of europium complex **1**. Conversely in the case of complex **2**, the emission intensity of the $^5D_0 \rightarrow {}^7F_2$ transition (612 nm) is approximately 3.6 times higher when excited at the ligand excitation maxima (313 nm) as compared to direct excitation at 394 nm. This indicates that ligand-to-europium energy transfer is effective in the case of europium complex **2**.

dx.doi.org/10.1021/ic2001249 |*Inorg. Chem.* 2011, 50, 4882–4891

Table 4. Radiative (A_{RAD}) and Nonradiative (A_{NR}) Decay Rates, $^5D_0/^5D_4$ Lifetimes (τ_{obs}), Radiative Lifetimes (τ_{RAD}), Intrinsic Quantum Yields (Φ_{Ln}), Energy Transfer Efficiencies (Φ_{sen}), and Overall Quantum Yields ($\Phi_{overall}$) for Complexes 1−4

Compounds	A_{RAD} (s^{-1})	A_{NR} (s^{-1})	τ_{obs} (μs)	τ_{RAD} (μs)	Φ_{Ln} (%)	Φ_{sen} (%)	$\Phi_{overall}$ (%)
1	944	1382	426 ± 2	1050 ± 2	41	3.6	1.5 ± 0.1[a]
			938 ± 2[c]				1.1 ± 0.1[b]
2	397	1938	426 ± 1	2518 ± 1	17	5.9	1.0 ± 0.2[a]
			886 ± 3[c]				0.9 ± 0.2[b]
3			1160 ± 7	1070 ± 11	~100	60	60 ± 6[a]
							58 ± 6[b]
4			1377 ± 1	1232 ± 14	~100	27	27 ± 3[a]
							24 ± 3[b]

[a] Absolute quantum yield. [b] Relative quantum yield. [c] τ_{obs} at 77 K.

Figure 8 summarizes the room temperature excitation spectra of complexes **3** and **4** in the solid state monitored around the more intense 545 nm emission line of the Tb^{3+} ion. These excitation spectra exhibit a large broad band in the 250−350 nm region which is associated with the electronic transitions of the ligands. The absence of any absorption bands due to f-f transitions of the Tb^{3+} cation proves that the luminescence sensitization via excitation of the ligand is effective.[10] The room temperature emission spectra of **3** and **4** (Figure 8) excited at 340 and 320 nm, respectively, exhibit a series of sharp lines which result from deactivation of the $^5D_4$ excited state to the corresponding ^7F_J ground state of the Tb^{3+} cation ($J = 6$, 5, 4, 3) centered at 488, 545, 585, and 620 nm.[5a,10,24] Moreover, the ligand-centered emission is not detected, thus implying the existence of an efficient ligand-to-metal energy transfer process in these complexes. Most importantly, the emission intensity of the Tb^{3+}-3,5-bis(benzyloxy)benzoate complex (**3**), especially at 545 nm, is found to be significantly higher (~2-fold) than that of the Tb^{3+}-3,5-bis(pyridine-2-ylmethoxy)benzoate complex (**4**).

The $^5D_0$ (Eu^{3+}) and $^5D_4$ (Tb^{3+}) decay curves were measured at both ambient (298 K) and low (77 K) temperatures and monitored within the more intense lines of the $^5D_0 \rightarrow {}^7F_2$ and $^5D_4 \rightarrow {}^7F_5$ transitions, respectively (See the Supporting Information, Figure S10−13), and the pertinent values are summarized in Table 4. The observed luminescence decay profiles correspond to single exponential functions at 298 and 77 K, thus implying the presence of only one emissive Eu^{3+} or Tb^{3+} center. The shorter $^5D_0$ lifetimes noted for Eu^{3+} complexes **1**−**2** (τ_{obs} = 0.426 ms) may be due to the dominant nonradiative decay channels associated with vibronic coupling on account of the presence of solvent molecules in the coordination spheres of these complexes. These values are essentially temperature dependent, with τ_{obs} (0.938 and 0.886 ms for **1** and **2**, respectively) approximately doubled in going from 298 to 77 K, thereby reflecting the presence of thermally activated deactivation processes. This effect has been well documented for several other hydrated Eu^{3+} carboxylate complexes.[5a,b,10] On the other hand, longer $^5D_4$ lifetime values at 298 K (τ_{obs} = 1.16 for **3** and 1.38 ms for **4**, respectively) have been observed for the Tb^{3+} complexes even when solvent molecules are present in the first coordination sphere since they are well-known to be vibrational deactivators of the excited states of Ln^{3+} ions.[5a,10] The energy gaps between the luminescent state and the ground state manifolds are approximately 12000 cm^{-1} and 14800 cm^{-1} for Eu^{3+} and Tb^{3+}, respectively. Relatively efficient coupling of the Eu^{3+} excited states occurs to the third vibrational overtone of the proximate OH oscillators ($\upsilon_{OH} \sim 3300-3500$ cm^{-1}), and to the fourth harmonic in the case of Tb^{3+}, which is consistent with the less efficient quenching observed in the case of Tb^{3+} where the Franck−Condon overlap factor is less favorable.[25] The $^5D_4$ lifetime values of Tb^{3+} complexes **3** and **4** are also found to be essentially temperature independent, with τ_{obs} varying by less than 1% while going from 298 to 77 K, thereby reflecting the absence of thermally activated deactivation processes.

To quantify the ability of the ligands designed to sensitize the luminescence of lanthanides, and to draw conclusions concerning the relationship between the structure and the properties, it was appropriate to analyze the emission in terms of eq 1 (below) where $\Phi_{overall}$ and Φ_{Ln}, represent the ligand-sensitized and intrinsic luminescence quantum yields of Ln^{3+}; Φ_{sen} represents the efficiency of the ligand-to-metal energy transfer and τ_{obs}/τ_{RAD} are the observed and the radiative lifetimes of Ln^{3+}.[26]

$$\Phi_{overall} = \Phi_{sen} \times \Phi_{Ln} = \Phi_{sen} \times (\tau_{obs}/\tau_{RAD}) \quad (1)$$

The intrinsic quantum yields of Eu^{3+} could not be determined experimentally upon direct f-f excitation because of very low absorption intensity.[1b] Therefore, the radiative lifetimes of Eu^{3+} ($^5D_0$) have been calculated from equation 2[26,27] where n represents the refractive index of the medium. An average index of refraction equal to 1.5 was employed in the calculation.[10] $A_{MD,0}$ is the spontaneous emission probability for the $^5D_0 \rightarrow {}^7F_1$ transition in vacuo (14.65 s^{-1}), and I_{tot}/I_{MD} signifies the ratio of the total integrated intensity of the corrected Eu^{3+} emission spectrum to the integrated intensity of the magnetic dipole $^5D_0 \rightarrow {}^7F_1$ transition:

$$1/\tau_{RAD} = A_{MD,0} \times n^3 \times (I_{tot}/I_{MD}) \quad (2)$$

The intrinsic quantum yield for Tb^{3+} (Φ_{Tb}) was estimated using eq 3 with the assumption that the decay process at 77 K in a deuterated solvent is purely radiative.[3b,25,28]

$$\Phi_{Tb} = \tau_{obs(298\ K)}/\tau_{obs(77\ K)} \quad (3)$$

Table 4 summarizes the radiative (A_{RAD}) and nonradiative (A_{NR}) decay rates, $\Phi_{overall}$, Φ_{Ln}, and Φ_{sen}. In the case of terbium luminescence, solid-state measurements gave a quantum yield of 60% for the Tb^{3+}-3,5-bis(benzyloxy)benzoate compound **3** compared with 27% for Tb^{3+}-3,5-bis(pyridine-2-ylmethoxy)-benzoate compound **4**. Conversely, the corresponding Eu^{3+} complexes **1**−**2** show poor luminescence efficiency with low quantum yields (1.5% for **1** and 1% for **2**). However, the present quantum yield, especially with Tb^{3+} coordination polymer constructed from 3,5-bis(benzyloxy)benzoate is found to be superior to that of recently reported Tb^{3+} coordination polymer of 3-methoxy-4-benzyloxy benzoate system ($\Phi_{overall}$ = 33%),[5a] and comparable with that of Tb^{3+}-coordination polymers assembled from β-diketonates and bidentate O-donor ligands

dx.doi.org/10.1021/ic2001249 |Inorg. Chem. 2011, 50, 4882–4891

($\Phi_{overall}$ = 56%),[4d] and Tb^{3+}-2,5-pyridinedicarboxylate system ($\Phi_{overall}$ = 45%).[5c] To better understand these results, one must take into account the $^3\pi\pi^*$-state energies of these ligands. According to the intramolecular energy transfer mechanism reported by Dexter and Sato et al.,[29] the intramolecular energy migration efficiency depends mainly on two energy transfer processes, namely, (i) the energy transfer from the lowest triplet energy level of the ligand to the resonant energy level of the lanthanide ion by Dexter's resonant exchange interaction; and (ii) the inverse energy transfer from Ln^{3+} ion to organic ligand by a thermal deactivation mechanism. If the energy difference is too small, the inverse energy transfer will take place much easier. Both energy transfer processes depend on the energy gap between the lowest triplet energy level of the organic ligand and the resonant energy level of the lanthanide ion. Clearly, there is an opposite influence between two energy transfer processes. Latva et al.'s empirical rule[19] states that an optimal ligand-to-metal energy transfer process for Tb^{3+} needs ΔE ($^3\pi\pi^*-{}^5D_4$) = 2500−4500 cm^{-1} and for Eu^{3+} ΔE ($^3\pi\pi^*-{}^5D_4$) = 2500−4000 cm^{-1}. On this basis it can be concluded that the energy transfer to the Tb^{3+} ion will be effective for the 3,5-bis(benzyloxy)benzoic acid and 3,5-bis(pyridine-2-ylmethoxy)-benzoic acid ligands, since ΔE ($^3\pi\pi^*-{}^5D_4$) for **3** and **4** are 4009 cm^{-1} and 4753 cm^{-1}, respectively. Complex **3** exhibits higher quantum yield ($\Phi_{overall}$ = 60%) and efficient ligand-to-metal energy transfer (Φ_{sen} = 60%) than complex **4** because of the superior match of the triplet energy level of the 3,5-bis(benzyloxy)benzoic ligand to that of the Tb^{3+} emitting level. On the other hand, poor sensitization efficiency for Eu^{3+} complexes has been noted for the above benzoate ligands mainly because of the larger energy gap between the triplet state and $^5D_0$ level of Eu^{3+} ΔE ($^3\pi\pi^*-{}^5D_0$) = 7259 cm^{-1} for **1** and 8003 cm^{-1} for **2**. Therefore, significantly lower quantum yields have been observed in Eu^{3+} complexes. Thus, it can be concluded that the derivatives of 3,5-dihydroxy benzoates are probably not suitable sensitizers for the excitation of Eu^{3+} ion.

CONCLUSIONS

Two new carboxylate ligands based on bis(benzyloxy)- and bis(pyridyl)-substituted 3,5-dihydroxy benzoic acids have been prepared from simple starting materials via a facile synthetic route. The new ligands form luminescent coordination polymers with trivalent lanthanides and sensitize their luminescence in the visible region. The following statements can be made regarding the structural and photophysical data of the new complexes:

(i) 3,5-Bis(pyridine-2-ylmethoxy)benzoic acid forms unique luminescent coordination polymers with both Eu^{3+} and Tb^{3+} ions. These polymers feature free Lewis basic pyridyl sites and may therefore prove to be useful for the sensing of heavy metal ions.

(ii) The newly designed benzoate ligands are adequate sensitizers for the Tb^{3+} ion. Indeed, their excited states lie at sufficiently high energies in comparison with that of the $^5D_4$ state to obviate back transfer of energy. As a result, even in the presence of metal-bound water molecules, the solid state quantum yields of the sensitized Tb^{3+} complexes are appreciable (as high as 60%). On the other hand, these ligands sensitize Eu^{3+} luminescence inefficiently, because of the larger energy gap between the triplet states of the ligands and $^5D_0$ level of Eu^{3+} ion.

Future studies, particularly those with 3,5-bis(pyridine-2-ylmethoxy)benzoic acid, will focus on the synthesis of luminescent complexes that are suitable for sensing of toxic metal ions.

ASSOCIATED CONTENT

Supporting Information. X-ray crystallographic data for complexes **2**, **4**, and **6** in CIF format, ^1H, ^{13}C NMR spectra for ligands, thermogravimetric data, powder XRD patterns for complexes **1**−**6**. Figures showing the coordination environments and intermolecular hydrogen bonding interactions of complexes **4** and **6**, and room temperature and low temperature luminescence decay profiles. Excitation spectrum of complex **5**. Emission spectra of **1** and **2** excited at different wavelengths (316, 362, 378, and 394 nm). A table for the infrared vibrational frequencies of the ligands and complexes, and a table containing absorption maxima and molar absorption coefficient data for the ligands and complexes. This material is available free of charge via the Internet at http://pubs.acs.org.

AUTHOR INFORMATION

Corresponding Author
*E-mail: mlpreddy55@gmail.com.

ACKNOWLEDGMENT

The authors acknowledge financial support from the Department of Science and Technology (SR/S1/IC-36/2007) and the Council of Scientific and Industrial Research (NWP0010). S.S.K. thanks CSIR, New Delhi, for the award of Junior Research Fellowship. A.H.C. thanks the Robert A. Welch Foundation (F-0003) for financial support.

REFERENCES

(1) (a) Eliseeva, S. V.; Bünzli, J.-C. G. *Chem. Soc. Rev.* **2010**, *39*, 189–227. (b) Bünzli, J.-C. G.; Piguet, C. *Chem. Soc. Rev.* **2005**, *34*, 1048–1077.

(2) (a) Bünzli, J.-C. G. *Chem. Rev.* **2010**, *110*, 2729–2755. (b) Kido, J.; Okamoto, Y. *Chem. Rev.* **2002**, *102*, 2357–2368. (c) de Bettencourt-Dias, A. *Dalton Trans.* **2007**, *22*, 2229–2241. (d) Tsukube, H.; Shinoda, S. *Chem. Rev.* **2002**, *102*, 2389–2403. (e) Brunet, E.; Juanes, O.; Rodriguez-Ubis, J. C. *Curr. Chem. Biol.* **2007**, *1*, 11–39.

(3) (a) Lehn, J. M. *Angew. Chem., Int. Ed.* **1990**, *29*, 1304–1319. (b) Sabbatini, N.; Guardiglia, M.; Lehn, J. M. *Coord. Chem. Rev.* **1993**, *123*, 201–228. (c) Piguet, C.; Bünzli, J.-C. G. *Chem. Soc. Rev.* **1999**, *28*, 347–358.

(4) (a) Binnemans, K. *Chem. Rev.* **2009**, *109*, 4283–4374. (b) Divya, V.; Biju, S.; Luxmi Varma, R.; Reddy, M. L. P. *J. Mater. Chem.* **2010**, *20*, 5220–5227. (c) Biju, S.; Reddy, M. L. P.; Cowley, A. H.; Vasudevan, K. V. *Cryst. Growth Des.* **2009**, *9*, 3562–3569. (d) Eliseeva, S. V.; Pleshkov, D. N.; Lyssenko, K. A.; Lepnev, L. S.; Bünzli, J.-C. G.; Kuzmina, N. P. *Inorg. Chem.* **2010**, *49*, 9300–9311.

(5) (a) Sivakumar, S.; Reddy, M. L. P.; Cowley, A. H.; Vasudevan, K. V. *Dalton Trans.* **2010**, *39*, 776–786. (b) Raphael, S.; Reddy, M. L. P.; Cowley, A. H.; Findlater, M. *Eur. J. Inorg. Chem.* **2008**, *28*, 4387–4394. (c) Soares-Santos, P. C. R.; Cunha-Silva, L.; Almeida Paz, F. A.; Sa Ferreira, R. A.; Rocha, J.; Trindade, T.; Carlos, L. D.; Nogueira, H. I. S. *Cryst. Growth Des.* **2008**, *8*, 2505–2516.

(6) (a) de Bettencourt-Dias, A.; Viswanathan, S. *Dalton Trans.* **2006**, *34*, 4093–4103. (b) Viswanathan., S.; de Bettencourt-Dias, A. *Inorg. Chem.* **2006**, *45*, 10138–10146.

(7) (a) Bredol, M.; Kynast, U.; Ronda, C. *Adv. Mater.* **1991**, *3*, 361–367. (b) Busskamp, H.; Deacon, G. B.; Hilder, M.; Junk, P. C.; Kynast, U. H.; Lee, W. W.; Turner, D. R. *CrystEngComm.* **2007**, *9*, 394–411. (c) Deacon, G. B.; Hein, S.; Junk, P. C.; Jüstel, T.; Lee, W.; Turner, D. R. *CrystEngComm.* **2007**, *9*, 1110–1123.

(8) (a) Raphael, S.; Biju, S.; Reddy, M. L. P.; Cowley, A. H.; Findlater, M. *Inorg. Chem.* **2007**, *46*, 11025–11030. (b) Remya, P. N.;

Biju, S.; Reddy, M. L. P.; Cowley, A. H.; Findlater, M. *Inorg. Chem.* **2008**, *47*, 7396–7404.

(9) (a) Zhong, R. Q.; Zou, R. Q.; Du, M.; Jiang, L.; Yamada, T.; Maruta, G.; Takeda, S.; Xu, Q. *CrystEngComm.* **2008**, *10*, 605–613. (b) Li, Y.; Zheng, F. K.; Liu, X.; Zou, W. Q.; Guo, G. C.; Lu, C. Z.; Huang, J. S. *Inorg. Chem.* **2006**, *45*, 6308–6316.

(10) Ramya, A. R.; Reddy, M. L. P.; Cowley, A. H.; Vasudevan, K. V. *Inorg. Chem.* **2010**, *49*, 2407–2415.

(11) (a) De Mello, C.; Wittmann, H. F.; Friend, R. H. *Adv. Mater.* **1997**, *9*, 230–232. (b) Palsson, L.-O.; Monkman, A. P. *Adv. Mater.* **2002**, *14*, 757–758. (c) Shah, B. K.; Neckers, D. C.; Shi, J.; Forsythe, E. W.; Morton, D. *Chem. Mater.* **2006**, *18*, 603–608.

(12) (a) Colle, M.; Gmeiner, J.; Milius, W.; Hillebrecht, H.; Brütting, W. *Adv. Funct. Mater.* **2003**, *13*, 108–112. (b) Saleesh Kumar, N. S.; Varghese, S.; Rath, N. P.; Das, S. *J. Phys. Chem. C* **2008**, *112*, 8429–8437.

(13) Eliseeva, S. V.; Kotova, O. V.; Gumy, F.; Semenov, S. N.; Kessler, V. G.; Lepnev, L. S.; Bünzli, J.-C. G.; Kuzmina, N. P. *J. Phys. Chem. A* **2008**, *112*, 3614–3626.

(14) Bril, A.; De Jager-Veenis, A. W. *J. Electrochem. Soc.* **1976**, *123*, 396–398.

(15) (a) Sheldrick, G. M. *SHELXTL-PC*, Version 5.03; Siemens Analytical X-ray Instruments, Inc.: Madison, WI, 1994. (b) Spek, A. L. *Acta Crystallogr., Sect. A.* **1990**, *C34*, 46.

(16) (a) Deacon, G. B.; Phillips, R. *J. Coord. Chem. Rev.* **1980**, *33*, 227–250. (b) Teotonio, E. E. S.; Brito, H. F.; Felinto, M. C. F. C.; Thompson, L. C.; Young, V. G.; Malta, O. L. *J. Mol. Struct.* **2005**, *751*, 85–94. (c) Soares-Santos, P. C. R.; Cunha-Silva, L.; Almeida Paz, F. A.; Ferreira, R. A. S.; Rocha, J.; Carlos, L. D.; Nogueira, H. I. S. *Inorg. Chem.* **2010**, *49*, 3428–3440.

(17) (a) Ye, J.; Zhang, J.; Ning, G.; Tian, G.; Chen, Y.; Wang, Y. *Cryst. Growth. Des* **2008**, *8*, 3098–3106. (b) Liu, M.-S.; Yu, Q.-Y.; Cai, Y.-P.; Su, C.-Y.; Lin, X.-M.; Zhou, X.-X.; Cai, J.-W. *Cryst. Growth. Des.* **2008**, *8*, 4083–4091.

(18) (a) Chen, J.-Q.; Cai, Y.-P.; Fang, H.-C.; Zhou, Z.-Y.; Zhan, X.-L.; Zhao, G.; Zhang, Z. *Cryst. Growth Des.* **2009**, *9*, 1605–1613. (b) Cai, Y.-P.; Zhang, H.-X.; Xu, A.-W.; Su, C.-Y.; Chen, C.-L.; Liu, H.-Q.; Zhang, L.; Kang, B.-S. *J. Chem. Soc., Dalton Trans.* **2001**, *16*, 2429–2434.

(19) Latva, M.; Takalo, H.; Mukkala, V. M.; Matachescu, C.; Rodriguez-Ubis, J. C.; Kanakare, J. *J. Lumin.* **1997**, *75*, 149–169.

(20) Steemers, F. J.; Verboom, W.; Reinhoudt, D. N.; Vander Tol, E. B.; Verhoeven, J. W. *J. Am. Chem. Soc.* **1995**, *117*, 9408–9414.

(21) (a) Gulgas, C. G.; Reineke, T. M. *Inorg. Chem.* **2005**, *44*, 9829–9836. (b) Zhang, L.; Xu, D.; Zhou, Y.; Jiang, F. *New J. Chem.* **2010**, *34*, 2470–2478. (c) Song, X.; Zhou, X.; Liu, W.; Dou, W.; Ma, J.; Tang, X.; Zheng, J. *Inorg. Chem.* **2008**, *47*, 11501–11513. (d) Bünzli, J.-C. G.; Charbonniére, L. J.; Ziessel, R. F. *J. Chem. Soc., Dalton Trans.* **2000**, 1917–1923. (e) Biju, S.; Ambili Raj, D. B.; Reddy, M. L. P.; Kariuki, B. M. *Inorg. Chem.* **2006**, *45*, 10651–10660. (f) Zucchi, G.; Olivier, M.; Pierre, T.; Gumy, F.; Bünzli, J.-C. G.; Michel, E. *Chem.—Eur. J.* **2009**, *15*, 9686–9696. (g) Ambili Raj, D. B.; Biju, S.; Reddy, M. L. P. *Inorg. Chem.* **2008**, *47*, 8091–8100.

(22) (a) Shavaleev, N. M.; Scopelliti, R.; Gumy, F.; Bünzli, J.-C. G. *Inorg. Chem.* **2009**, *48*, 6178–6191. (b) Shavaleev, N. M.; Eliseeva, S. V.; Scopelliti, R.; Bünzli, J.-C. G. *Chem.—Eur. J.* **2009**, *15*, 10790–10802.

(23) (a) Ambili Raj, D. B.; Francis, B.; Reddy, M. L. P.; Butorac, R. R.; Lynch, V. M.; Cowley, A. H. *Inorg. Chem.* **2010**, *49*, 9055–9063. (b) Francis, B.; Ambili Raj, D. B.; Reddy, M. L. P. *Dalton Trans.* **2010**, *39*, 8084–8092.

(24) Biju, S.; Reddy, M. L. P.; Cowley, A. H.; Vasudevan, K. V. *J. Mater. Chem.* **2009**, *19*, 5179–5187.

(25) (a) Dossing, A. *Eur. J. Inorg. Chem.* **2005**, *8*, 1425–1434. (b) Beeby, A.; Clarkson, I. M.; Dickins, R. S.; Faulkner, S.; Parker, D.; Royle, L.; de Sousa, A. S.; Williams, J. A. G.; Woods, M. *J. Chem. Soc. Perkin Trans. 2* **1999**, *3*, 493–503.

(26) (a) Shavaleev, N. M.; Eliseeva, S. V.; Scopelliti, R.; Bünzli, J.-C. G. *Inorg. Chem.* **2010**, *49*, 3927–3936.

(27) Werts, M. H. V.; Jukes, R. T. F.; Verhoeven, J. W. *Phys. Chem. Chem. Phys.* **2002**, *4*, 1542–1548.

(28) Nasso, I.; Bedel, S.; Galaup, C.; Picard, C. *Eur. J. Inorg. Chem.* **2008**, 2064–2074.

(29) (a) Dexter, D. L. *J. Chem. Phys.* **1953**, *21*, 836–851. (b) Brown, T. D.; Shepherd, T. M. *J. Chem. Soc., Dalton Trans.* **1973**, *3*, 336–341.